

# Pumping optimization of coastal aquifers using probabilistic search – case study: Quaternary aquifer of El-Arish Rafah, Egypt

Hamdy A. El-Ghandour and Emad Elbeltagi

## ABSTRACT

The increased pumping of freshwater from coastal aquifers, to meet growing demands, causes an environmental problem called saltwater intrusion. Consequently, proper management schemes are necessary to tackle such a situation and permit the optimal development of coastal groundwater basins. In this research, a probabilistic search algorithm, namely Probabilistic Global Search Lausanne (PGSL), is used to calculate optimal pumping rates of unconfined coastal aquifer.

The results of using PGSL are compared with a stochastic search optimization technique, Shuffled Frog Leaping Algorithm (SFLA). The finite element method is applied to simulate the hydraulic response of the steady state homogenous aquifer. The lower and upper (LU) decomposition method is adapted to invert the conductance matrix, which noticeably decreases the computation time. The results of both the PGSL and the SFLA are verified through the application on the aquifer system underlying the City of Miami Beach in the north of Spain. Multiple independent optimization runs are carried out to provide more insightful comparison outcomes. Consequently, a statistical analysis is performed to assess the performance of each algorithm. The two optimization algorithms are then applied on the Quaternary aquifer of El-Arish Rafah area, Egypt. The results show that both algorithms can effectively be used to obtain nearly global solutions compared with other previous published results.

**Key words** | finite elements, Probabilistic Global Search Lausanne, Quaternary aquifer, saltwater intrusion, sharp interface assumption, Shuffled Frog Leaping Algorithm

**Hamdy A. El-Ghandour** (corresponding author)  
Irrigation and Hydraulics Department,  
Faculty of Engineering,  
Mansoura University,  
Mansoura 35516,  
Egypt  
E-mail: [hamdy\\_elghandour@yahoo.com](mailto:hamdy_elghandour@yahoo.com)

**Emad Elbeltagi**  
Structural Engineering Department,  
Faculty of Engineering,  
Mansoura University,  
Mansoura 35516,  
Egypt

## INTRODUCTION

Groundwater contamination through saltwater intrusion threatens the health of many people living in coastal areas. Coastal aquifers in arid and semi-arid zones which border the sea are an important source for water. Coastal areas are usually heavily urbanized zones, a fact that makes the need for freshwater even more acute. To meet growing demands, increased freshwater is extracted from these aquifers. Consequently, wells used for freshwater may be contaminated by saltwater intrusion.

In recent decades, stochastic optimization combined with flow simulation has been widely used to control saltwater intrusion and the general management of coastal groundwater. In most previous coastal groundwater management studies, simulated flow models are based on numerical methods such as the Finite Difference Method (FDM) (Bakker 2003) and the Finite Element Method (FEM) (El-Alfy *et al.* 2015) or analytical methods such as the theory of images (Abdel-Gawad & Shamaa 2004). The use of numerical or analytical methods for coastal aquifer simulation along with optimization algorithms is constrained by the huge computational burden involved. These approaches differ in the used methods to simulate the coastal groundwater flow system, the type of

This is an Open Access article distributed under the terms of the Creative Commons Attribution Licence (CC BY 4.0), which permits copying, adaptation and redistribution, provided the original work is properly cited (<http://creativecommons.org/licenses/by/4.0/>).

doi: 10.2166/nh.2019.093

groundwater management problems and the algorithms used to solve these problems. Different objective functions and constraints have been employed to control this problem such as total pumping rate maximization, drawdown minimization, pumped water salinity minimization and pumping cost (Javadi *et al.* 2015; Christelis & Mantoglou 2018; Yang *et al.* 2018). In simulation–optimization modeling, the objective function is evaluated using an optimization algorithm, while the simulation model is utilized to satisfy the constraints.

Studies of the application of stochastic optimization algorithms for the management of coastal aquifers are reported in the literature. Cheng *et al.* (2000) reported the first application of the structured messy genetic algorithm (GA) combined with analytical solutions. GA and its variants are the most popular of stochastic optimization methods for such problems (Abd-Elhamid & Javadi 2011; Javadi *et al.* 2015). Examples of other applications include particle swarm optimization (Karatzas & Dokou 2015), ant colony optimization (Ataie-Ashtiani & Ketabchi 2011), differential evolution (Elçi & Ayvaz 2014), simulated annealing (Rao *et al.* 2004), and simplex simulated annealing (Kourakos & Mantoglou 2009). The literature review shows that some optimization algorithms were rarely used in groundwater resources management and, to the authors' knowledge, there is no report of the application of the Shuffled Frog Leaping Algorithm (SFLA) for coastal groundwater management.

Decision variables are related to pumping rate schemes (Cheng *et al.* 2000; Ataie-Ashtiani & Ketabchi 2011), water table level or drawdown (Katsifarakis & Tselepidou 2009), well locations (Elçi & Ayvaz 2014), the salinity of pumped water from wells (Ataie-Ashtiani *et al.* 2014), saltwater volume into the aquifer (Emch & Yeh 1998), operating costs (Abd-Elhamid & Javadi 2011), net benefits (Ferreira da Silva & Haie 2007), recharge rate schemes (Kourakos & Mantoglou 2011), trade-off between environmental and social issues, and interactions between surface and subsurface resources. Constraints include pumping limits (Cheng *et al.* 2000; Rao *et al.* 2004; Katsifarakis & Petala 2006), saltwater toe location (Cheng *et al.* 2000; Ferreira da Silva & Haie 2007; Ataie-Ashtiani & Ketabchi 2011), salt concentration (Kourakos & Mantoglou 2011; Ataie-Ashtiani *et al.* 2014), water table level (Katsifarakis & Tselepidou 2009), strategic nature of the aquifer, existing infrastructures, and historical rights rates (Abarca *et al.* 2006).

Over the years, a large number of models have been developed and used to study saltwater intrusion in coastal aquifers. FDM and FEM are widely used to simulate the groundwater flow. These models are SUTRA (Ojeda *et al.* 2004), SEAWAT (Kopsiaftis *et al.* 2017, 2019), CODESA-3D (Paniconi *et al.* 2001), SWIFT (Ma Tain *et al.* 1997), MOCDENS3D (Oude Essink 2001), SHARP (Barreto *et al.* 2001), Quasi-three-dimensional finite element (Zhou *et al.* 2003), and SHEMAT (Scholze *et al.* 2002).

Probabilistic Global Search Lausanne (PGSL) is a global search algorithm proposed by Raphael & Smith (2003a). It depends on selective sampling of the search space using a probability density function (PDF) that is varied dynamically during the search process. PGSL starts with a population of random solutions and ranks them based on their objective function values. Regions that contain good solutions, having higher probabilities, are searched with greater intensity. The application of PGSL on many benchmark problems with multi-variable non-linear objective functions demonstrated that PGSL performs better than GA, and simulated annealing (Raphael & Smith 2003b). There are a few applications of PGSL for water resources management such as minimum cost design of irrigation canals (Adarsh 2012; Adarsh & Sahana 2013), however it is not used in the literature for coastal groundwater management.

The objective of the current study is to calculate the optimal pumping rates in an unconfined coastal aquifer under steady-state conditions and assuming a sharp saltwater interface. Simulation-optimization models are developed using both the PGSL and SFLA optimization algorithms combined with FEM on Strack's (1976) formulation to simulate the groundwater flow. The results of the two optimization algorithms are compared. Both methods are then verified through their application on the aquifer system under the City of Miami Beach in northern Spain. Finally, they are applied to the Quaternary aquifer of El-Arish Rafah, Egypt.

---

## OPTIMIZATION OF PUMPING RATES FROM COASTAL AQUIFERS

In this paper, the management strategy is settled to either maximize the economic benefit from the pumped water (Equation (1)) or maximize the total pumping of fresh water (Equation

(2). The pumping rates from a pre-existing system of wells of known locations are considered as the problem decision variables. The management strategy can be stated mathematically for each case as follows (Benhachmi *et al.* 2003):

$$\text{maximize } f_1(Q_1, Q_2, \dots, Q_{nw}) = \sum_{i=1}^{nw} Q_i [B - C(L_i - h_i)] \quad (1)$$

$$\text{maximize } f_2(Q_1, Q_2, \dots, Q_{nw}) = \sum_{i=1}^{nw} Q_i \quad (2)$$

in which,  $f_1$  and  $f_2$  are the objective functions of maximum benefit and maximum pumping respectively;  $Q$  is the well pumping rate;  $B$  is the economic benefit for one cubic meter of fresh water;  $C$  is the cost of lifting one cubic meter of water per one meter height;  $L_i$  is the ground level from a specified datum;  $h_i$  is the water table from a specified datum; and  $nw$  is the number of wells.

Figure 1 shows a sketch of saltwater intrusion in a coastal unconfined aquifer. The groundwater flow is described by Equation (3a) and (3b) (Hunt 1983):

for freshwater (zone I)

$$\frac{\partial}{\partial x} \left( kh \frac{\partial h}{\partial x} \right) + \frac{\partial}{\partial y} \left( kh \frac{\partial h}{\partial y} \right) = \sum_{i=1}^{nw} \delta(x - x_i) Q_i \delta(y - y_i) \quad (3a)$$

for saltwater (zone II)

$$\frac{\partial}{\partial x} \left( k \frac{(h-d)}{\varepsilon} \frac{\partial h}{\partial x} \right) + \frac{\partial}{\partial y} \left( k \frac{(h-d)}{\varepsilon} \frac{\partial h}{\partial y} \right) = \sum_{i=1}^{nw} \delta(x - x_i) Q_i \delta(y - y_i) \quad (3b)$$

in which  $h$  is the vertically averaged piezometric head (measured from the impervious bed of the aquifer, Figure 1);  $k$  is the hydraulic conductivity;  $\varepsilon = (\rho_s - \rho_f)/\rho_s$ ;  $\rho_s$  and  $\rho_f$  are the densities of saltwater and freshwater;  $d$  is the elevation of mean sea level (M.S.L.) above the impervious bed of the aquifer;  $Q_i$  is the rate of freshwater pumping from well  $i$  located at coordinates  $(x_i, y_i)$ ; and  $\delta(z)$ : the Dirac delta function equals one if  $z$  equals zero otherwise equals zero.

In this study, for the unconfined aquifer, the following assumptions are considered (Figure 1): (1) sharp interface between saltwater and freshwater, (2) the three-dimensional geometry flow equation is reduced to two-dimensional by Dupuit's assumption, (3) steady-state flow condition, (4)

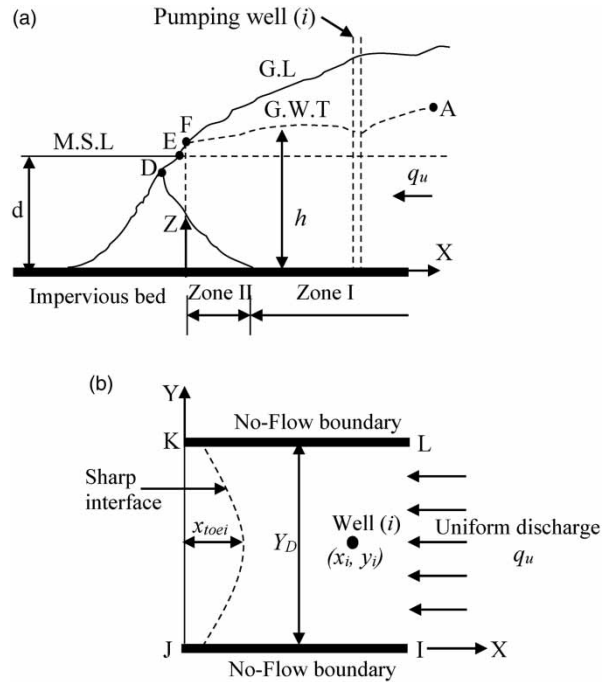


Figure 1 | Definition sketch of saltwater intrusion in coastal unconfined aquifer. (a) Sectional view for unconfined aquifer. (b) Plan of the studied domain.

the Ghyben–Herzberg assumption is utilized to interpret the interface location, (5) wells fully penetrate the aquifer thickness, (6) horizontal impervious aquifer bed, and (7) wells are only within the fresh water zone.

Strack (1976) presented a derivation to transform the nonlinear Equation (3a) and (3b) to a precise linear form (Equation (4)). Consequently, the dependent variable  $h$  has to be replaced with potential  $\phi$ , for both zones I and II (Cheng *et al.* 2000).

$$\frac{\partial}{\partial x} \left( k \frac{\partial \phi}{\partial x} \right) + \frac{\partial}{\partial y} \left( k \frac{\partial \phi}{\partial y} \right) = \sum_{i=1}^{nw} \delta(x - x_i) Q_i \delta(y - y_i) \quad (4)$$

in which  $\phi = (h^2 - sd^2)/2$  for zone I,  $\phi = (h - d)^2/2\varepsilon$  for zone II,  $s = \rho_s/\rho_f$ , and the two zones separated at  $\phi_{toe} = s(s - 1)d^2/2$ .

The set of constraints are (Figure 1):

$$\frac{\partial \phi_j}{\partial n} = 0 \quad \forall j \in \text{sides IJ, LK} \quad (5)$$

$$\frac{\partial \phi_j}{\partial n} = \frac{q_u}{k} \quad \forall j \in \text{side IL} \quad (6)$$

$$\phi_j = \overline{FE}^2 / 2\varepsilon \quad \forall j \in \text{side JK} \quad (7)$$

$$\phi_j > 0 \quad \forall j \in N_n \quad (8)$$

$$x_{toei} < x_i \quad \forall i \in nw \quad (9)$$

$$Q_{\min i} \leq Q_i \leq Q_{\max i} \quad \forall i \in nw \quad (10)$$

in which  $q_u$  is defined as the aquifer uniform rate of discharge per unit width;  $\overline{FE}$  is the unconfined aquifer freshwater seepage face above the M.S.L, calculated as  $\overline{FE} = q_{net}/K$  (Hunt 1983);  $q_{net}$  is the net uniform discharge flow to the sea and is equal to  $(q_u \times Y_D - \sum_{i=1}^{nw} Q_i)$ ;  $N_n$  is the number of nodes through the discretized domain JILK;  $x_{toei}$  is the intrusion length at  $y_i$  where  $y_i$  is the y coordinate of well  $i$ ;  $x_i$  is the horizontal coordinate of well  $i$  (Figure 1(b));  $Q_i$  is the pumping rate of well  $i$ ; and  $Q_{\min i}$  and  $Q_{\max i}$  are the minimum and maximum permissible pumping rates corresponding to well  $i$ .

The seepage faces around different wells are ignored within the present study.

FEM is applied to discretize Equation (4) within the coastal aquifer JILK (Figure 1). Then, the FEM is transformed to a set of linear equations as follows:

$$[Stiff] \times [\phi] = [F] \quad (11)$$

in which  $[Stiff]$  is the stiffness/conductance square matrix with dimensions of  $N_n \times N_n$ ,  $[\phi]$  is the unknown vector of dimension  $N_n \times 1$ , and  $[F]$  is the load vector including both pumped or recharged water. Finally, Equation (11) is rearranged to simplify its use (Equation (12)) by calculating the inverse of the  $[Stiff]$  matrix using the LU-decomposition method.

$$[\phi] = inv[Stiff] \times [F] \quad (12)$$

## PROBABILISTIC GLOBAL SEARCH LAUSANNE ALGORITHM

PGSL is a search algorithm based on sampling of the search space, without using special operators, using a probability distribution function (PDF) defined over the entire search space (Raphael & Smith 2003b). Potential solutions are generated randomly and evaluated using a defined objective. The basic

assumption is that good solutions are more likely to be found in the regions with higher probabilities. Hence, the search is concentrated in regions containing good solutions. The evolution of solutions is carried out through updating the PDF in regions where good solutions are found. Unlike other techniques, there is no point-to-point movement towards a global optimum solution. Instead PGSL relies on a sampling procedure similar to the Monte-Carlo technique. In the beginning, each variable range (maximum value – minimum value) is divided into a number of intervals and a uniform probability is assumed within each interval. As the search progresses, intervals containing good solutions are assigned higher probability values and the search space along the variable is narrowed. As such, the search space is gradually narrowed down until convergence is achieved. The algorithm includes four nested cycles named Sampling, Probability updating, Focusing, and Sub-domain. The PGSL involves the following steps:

1. Initialization: The PDF of each decision variable is assumed having a uniform distribution over the entire domain.
2. Sampling cycle: Solutions are generated randomly using the current PDF. Then, each solution is evaluated and the best solution is selected.
3. Probability updating cycle: In this cycle, each decision variable PDF is modified using the probability-updating algorithm. This ensures that the probabilities of regions containing good solutions are increased.
4. Focusing cycle: After each iteration, the search is then focused on the interval containing the best point. For each decision variable, the interval containing the best point is then subdivided into smaller intervals.
5. Sub-domain cycle: At the beginning the entire space is searched, while in subsequent iterations a sub-domain of the problem is selected for search. The sub-domain size gradually decreases by changing the minimum and maximum values of each variable until the solution converges to a point.

The main parameters of the PGSL algorithm are: the number of evaluations of the objective function (*numeval*), number of focusing cycles (*NFC*) equals  $20 \times \text{number of variables}$  (Raphael & Smith 2003b), number of probability updating cycles (*NPUC*), Number of sampling cycles (*NSC*), and number of sub-domain cycles (*NSDC*) equals integer of

$numeval/(NSC \times NPUC \times NFC)$  (Raphael & Smith 2003b). The flowchart describing the PGSL algorithm is shown in Figure 2.

### SHUFFLED FROG LEAPING ALGORITHM

SFLA is used to seek a global optimal solution of combinatorial optimization problems. It combines the benefits of the idea of mixing information from parallel local searches and the social behavior-based particle swarm optimization algorithms to move towards a global solution. In this algorithm, the generation of a number of memplexes is carried out, each one containing a number of random frogs (solutions). The frogs with the best fitness ( $X_B$ ) and the worst fitness ( $X_W$ ) in each memplex are determined. Also, in each cycle of evolution, the frog having the global best fitness ( $X_G$ ) is determined and the worst fitness frog is updated. The SFLA involves the following steps:

1. Random initialization of initial population of possible solutions.
2. The fitness of each solution is calculated based on the given objective function and constraints violation penalties.
3. Determination of the global best frog position ( $X_G$ ).
4. Population is partitioned into subsets named memplexes representing different cultures of frogs. Then, the following steps are carried out for each memplex:
  - Determine both the best and worst frog positions (i.e.  $X_B$  and  $X_W$ ).
  - Update the worst frog position using Equations (13) and (14) (Elbeltagi *et al.* 2007):

$$D(l) = c \times r \times [X_B(l) - X_W(l)],$$

$$D_{max} \geq D_l \geq -D_{max}, \quad \forall l \in n_m \quad (13)$$

$$X_{Wnew}(l) = X_{Wcurrent}(l) + D(l), \quad \forall l \in n_m \quad (14)$$

in which  $D(l)$  is a change in the position of the worst frog,  $X_W(l)$ , located in memplex  $l$ ,  $X_B(l)$  is the position of the best frog located in memplex  $l$ ,  $X_{Wnew}(l)$  is the worst frog new position located in memplex  $l$ ,  $X_{Wcurrent}(l)$  is the worst frog current position located in memplex  $l$ ;  $c$  is a search acceleration factor proposed by Elbeltagi *et al.* (2007),  $r$  is a random number ranging from 0 to 1,  $n_m$  is the number of

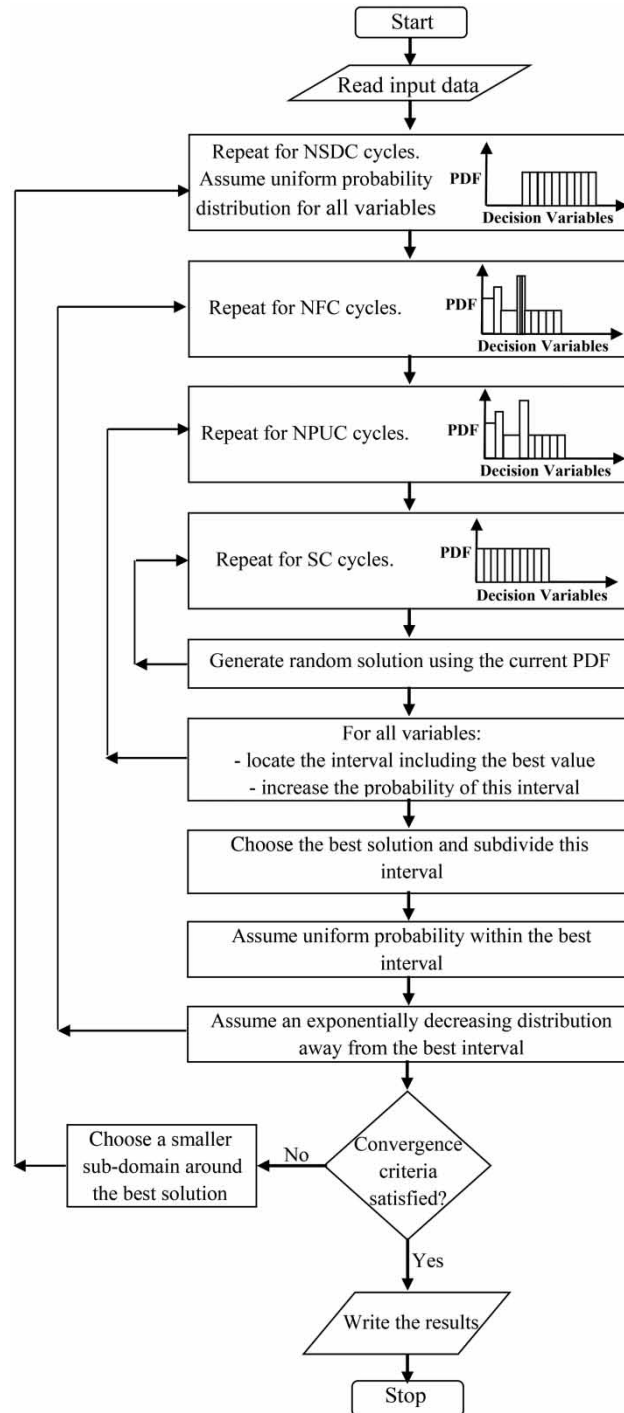


Figure 2 | Flowchart of the PGSL algorithm.

memplexes and  $D_{max}$  is the maximum allowed change in the worst frog position.

- If the obtained new position is better than the worst, change the worst frog with the new one. Otherwise,

re-apply both Equations (13) and (14) replacing XB (l) by XG.

- If the obtained new position is better than the worst, change the worst frog with the new one. Otherwise, generate a new frog randomly.
5. Perform step (4) for a specified number of trials until the position of the worst frog is improved.
  6. Shuffling process is carried out for all frog positions in all memplexes.
  7. Steps 2–6 are repeated until no improvement occurs in the global best frog position (best solution).

The main parameters of the SFLA are: number of frogs, number of memplexes, trials before shuffling and number of iterations after shuffling, maximum allowed change in frog position  $D_{max}$ , and the search acceleration factor  $c$  value. The flowchart describing the steps of SFLA is presented in Figure 3.

## MODEL VERIFICATION

The PGSL and SFLA optimization algorithms are verified through applying them on a well-known benchmark problem. At the same time, the results of both models are compared. The two optimization models used the FEM to simulate the flow in coastal aquifers. The two algorithms are applied on the unconfined coastal aquifer at Miami Beach in the north of Spain (Benhachmi *et al.* 2003) to maximize both the net benefit on one scenario and maximize the total pumping on another scenario. In the two scenarios, pumping rates from a pre-existing system of wells are considered as the decision variables. The studied unconfined aquifer is considered among the most important sources of water supply for the city of Miami Beach. The Miami coastal aquifer consists of single-layered unconsolidated sediment of Quaternary age with pore permeability corresponding to coastal piedmonts and alluvial fans. The sediments consist of clay and gravel, and overlay blue clay of Pliocene age, constituting the effective lower impervious hydrologic boundary. The hydraulic parameters of the studied aquifer are its length along the sea coast ( $Y_D = 5,000$  m) and perpendicular to the sea cost equals 4,500 m, hydraulic conductivity ( $K = 14$  m/d), uniform discharge per unit width of the aquifer ( $q_u = 1.2$  m<sup>3</sup>/d/m), depth of impervious bed from M.S.L.

( $d = 30$  m), saltwater density ( $\rho_s = 1,025$  kg/m<sup>3</sup>), and freshwater density ( $\rho_f = 1,000$  kg/m<sup>3</sup>) (Benhachmi *et al.* 2003). Table 1 shows the coordinates of the aquifer pre-existing wells, their allowable maximum and minimum pumping rates, and their corresponding ground level.

### Scenario 1: maximizing the economic benefit

The management strategy is settled to maximize the economic benefits from the pumped water and to minimize the cost corresponding to lifting the water, Equation (1). The values  $B$  and  $C$  shown in Equation (1) equal 0.01 \$/m<sup>3</sup> and 0.0002 \$/m<sup>3</sup>/m respectively (Benhachmi *et al.* 2003). In Miami Beach there is a region near the sea coast with confined conditions and a groundwater level higher than the ground level (Abdel-Gawad & Shamaa 2004). Consequently, in cases where the water level is higher than the ground level, the value of the constant  $C$  is set equal to zero. Several trial runs are carried out to determine both the suitable parameters' values of the SFLA and the PGSL (Table 2). The largest values obtained for the net benefit (Equation (1)) are 24.93 and 23.07 \$/d for both the SFLA and PGSL with corresponding total pumping rates equal to 3,849.4 and 3,999.8 m<sup>3</sup>/d, respectively. The obtained values of pumping rates represent 64.2 and 66.7% for the SFLA and PGSL of the total water entering the aquifer, respectively. The corresponding total numbers of the objective function evaluations, Equation (1), are 19,946 and 2,000 for the SFLA and the PGSL, respectively. Table 3 compares the discharge of each well corresponding to the largest obtained net benefits of the two models in the current study and other previous studies. It is noticed that most of the water is withdrawn from wells having low ground level to decrease the lifting cost of pumped water. As reported in Table 3, the SFLA gives a higher value for the benefit in comparison with the two previous studies while the PGSL gives a close value for the higher reported value. Also, it is found that the economic benefits obtained from the SFLA are larger than those obtained from the PGSL which has a higher total pumping rate.

### Scenario 2: maximize the total pumping

In this scenario, the unconfined aquifer under Miami Beach is restudied to maximize the total pumping of freshwater, Equation (2). After performing several trial runs, the suitable

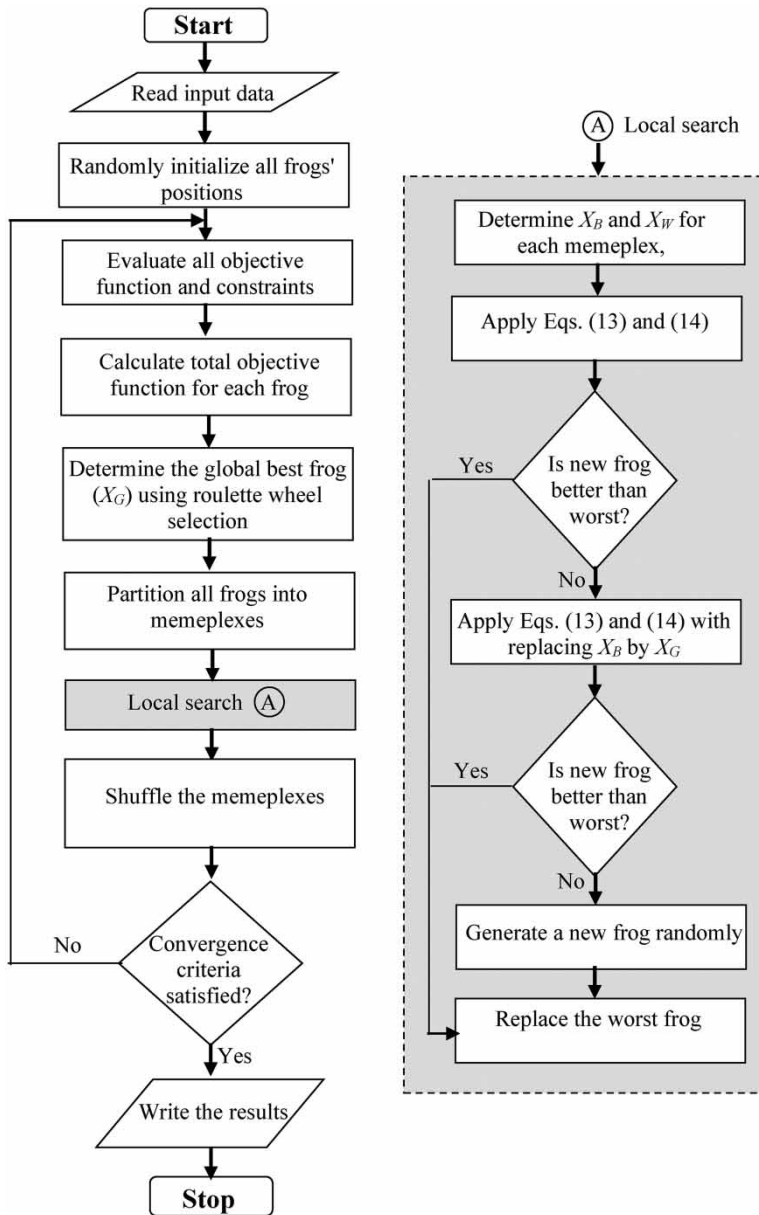


Figure 3 | Flowchart of the single-objective SFLA.

values of SFLA and PGSL parameters are listed in Table 2. The largest total pumping rates obtained are 5,427.8 and 5,310.2 m<sup>3</sup>/d, respectively, for both the SFLA and PGSL that represent about 90.5 and 88.5% of the total water entering the aquifer. The corresponding total numbers of evaluations of the objective function, Equation (2), are 64,079 and 2,000 for the SFLA and PGSL, respectively. Table 4 presents a comparison between the discharge of each well corresponding to the largest total pumping of the two models in the current study

and previous studies. As presented in the table, Abdel-Gawad & Shamaa (2004) obtained the largest total pumping rates. However, when checking the well pumping rates given by Abdel-Gawad & Shamaa (2004) against both constraints shown in Equations (8) and (9) using the developed FEM simulation method, it was found that seawater had intruded into several wells (Table 4). This may be due to the different method they adopted (the theory of images) to simulate the hydraulic response in the aquifer or due to the incorrect

**Table 1** | Miami Beach unconfined aquifer data

Well no.	X (m)	Y (m)	Max. pumping rate (m <sup>3</sup> /d)	Min. pumping rate (m <sup>3</sup> /d)	Ground level (m)
1	3,877.26	4,361.68	1,200.0	120.0	79.798
2	3,825.54	3,747.51	1,200.0	120.0	112.869
3	3,654.91	3,390.29	1,200.0	120.0	110.598
4	3,625.24	2,647.67	1,000.0	120.0	89.0
5	3,507.27	3,686.34	1,200.0	120.0	80.685
6	3,469.01	3,899.55	1,200.0	120.0	78.414
7	3,285.2	4,148.47	1,200.0	120.0	66.077
8	3,160.71	4,714.84	1,000.0	120.0	66.946
9	3,133.13	2,592.51	1,000.0	120.0	85.0
10	2,807.67	960.58	900.0	120.0	90.66
11	2,743.8	2,705.04	1,000.0	120.0	70.0
12	2,647.26	758.77	900.0	120.0	89.156
13	2,046.9	2,495.63	1,200.0	120.0	65.0
14	1,322.07	2,922.15	300.0	120.0	25.0
15	1,245.52	2,540.73	300.0	120.0	30.0
16	1,077.24	2,768.99	300.0	120.0	22.0
17	905.54	2,761.39	300.0	120.0	19.0
18	872.59	4,202.28	300.0	120.0	20.0
19	703.79	762.84	300.0	120.0	34.0

**Table 2** | Values of the parameters used in the verification and application cases

Model	Parameter names	Miami Beach	El-Arish Rafah Beach
PGSL	- NSDC:	2	1
	- NFC:	380	620
	- NPUS:	1	1
	- NSC:	2	2
	- numeval:	2,000	2,000
SFLA	- number of frogs:	100	100
	- number of memplexes:	10	10
	- number of trials before shuffling:	20	20
	- number of iterations after shuffling:	10	10
	- the maximum change in frog position $D_{max}$ :	900, 300 <sup>a</sup>	10,000
	- the search acceleration factor $c$ :	4.2	4.2

<sup>a</sup>The first value corresponds to the first 13 wells while the second value is for the remaining wells.

**Table 3** | Pumping rates from well system in Miami Beach corresponding to scenario 1 using different optimization techniques

Well no.	Abdel-Gawad & Shamaa (2004)	El-Ghandour (2005)	The present study	
	GA	GA	SFLA	PGSL
1	0	365.2	0	0
2	0	0	0	0
3	0	0	0	0
4	0	0	0	0
5	0	0	0	0
6	120.0	0	0	254.8
7	958.7	504.5	900.0	575.0
8	491.9	545.0	497.8	171.1
9	0	355.1	0	0
10	0	0	0	0
11	0	161.9	0	882.6
12	0	0	0	0
13	675.2	697.5	651.5	479.8
14	300.0	249.4	300.0	278.3
15	300.0	138.9	300.0	283.0
16	275.0	115.5	300.0	299.6
17	218.6	225.6	300.0	197.6
18	300.0	299.4	300.0	284.9
19	300.0	269.6	300.0	293.1
Maximum benefit (\$/d)	23.81	21.25	24.93	23.07
Total pumping rates (m <sup>3</sup> /d)	3,939.4	3,927.6	3,849.4	3,999.8

number of mirrors used to represent the theory of images. However, the two developed models also presented a good solution for the total pumping with the SFLA outperforming the PGSL.

As such, both the PGSL and SFLA optimization algorithms are able to reach greater solutions without violating the constraints when compared to previous studies.

### COMPARISON OF THE TWO OPTIMIZATION ALGORITHMS' PERFORMANCE

The methodology adopted in the comparison of the two optimization algorithms' performance begins by performing 20 consecutive trial runs corresponding to each one. Then, a comparison is carried out between both based on a set of criteria, namely: (1) the success rate,  $S_r$  [ $=(N_s/N_t) \times 100$ ] (where



**Table 4** | Pumping rates from well system in Miami Beach corresponding to scenario 2 using different optimization techniques

Well no.	Abdel-Gawad & Shamaa (2004)	El-Ghandour (2005)	The present study	
	GA	GA	SFLA	PGSL
1	533.9	453.6	900.0	370.7
2	528.1	231.1	0	0
3	479.0	381.6	0	127.6
4	766.2	362.4	0	794.7
5	263.6 <sup>a</sup>	580.6	0	704.2
6	347.9 <sup>a</sup>	0	900.0	0
7	280.0 <sup>a</sup>	164.6	0	0
8	309.1 <sup>a</sup>	558.6	513.6	790.8
9	463.3	389.9	900.0	0
10	554.8	448.7	900.0	706.2
11	282.9	558.7	542.6	735.5
12	480.7	529.2	595.0	761.4
13	171.2 <sup>a</sup>	457.1	176.7	319.1
14	0	0	0	0
15	0	0	0	0
16	0	0	0	0
17	0	0	0	0
18	0	0	0	0
19	0	0	0	0
Total pumping rates (m <sup>3</sup> /d)	5,460.7	5,116.1	5,427.8	5,310.2

<sup>a</sup>Intruded well.

$N_s$  is the number of trials each model succeeds, to catch a value for the objective function greater than the maximum corresponding value reported in the literature and  $N_t$  is the total number of trials; (2) the minimum, maximum, mean, and standard deviation of the obtained solutions; and (3) mean *numeval*. The maximum values of the objective functions reported in the literature are 23.81 \$/d and 5,116.1 m<sup>3</sup>/d respectively for scenarios 1 and 2 without constraints violations (feasible solution). It is worth noting that for fair comparison, the run time for each trial for both algorithms is kept constant (i.e. 45 minutes); this time was selected based on the recorded average run time during the previous experiments. The evaluation criteria values associated with both scenario 1 (i.e. maximization of economic benefit) and scenario 2 (i.e. maximization of total pumping rates) for the two developed models are summarized and presented in Table 5. From this table it is seen that the SFLA has the highest success

rate, for the two scenarios of a value equal to 90% for scenario 1. This means that the SFLA is able to catch an optimal solution for the economic benefit greater than the corresponding maximum value reported in the literature for 18 runs out of the 20 carried runs. Also, the SFLA has higher minimum, maximum, and mean values for the two scenarios. The smaller standard deviation of the objective function is corresponding to the PGSL in both scenarios, with a value of 0.52 for scenario 1 and 116.3 for scenario 2. Consequently, the performance of the SFLA is better than the PGSL in terms of the success rate, minimum, maximum, and mean values for the two scenarios. The PGSL performed better in terms of standard deviation of the objective function for both scenarios. The mean *numeval* for the PGSL was significantly smaller than the SFLA in the two scenarios. In scenario 2, for example, the mean *numeval* for the PGSL was 3,753 while it was 23,654 for the SFLA. Thus, the PGSL would be very beneficial, especially when the number of variables increases, as the processing time increases exponentially.

Although the SFLA performs better than the PGSL, the latter outperforms other models reported in the literature.

## APPLICATION OF THE DEVELOPED MODELS TO EL-ARISH RAFAH AQUIFER, EGYPT

The Quaternary aquifer in north Sinai consists of three areas, namely: the area from Rafah to east of El-Arish, the Delta El-Arish valley and the area from Bir El-Abd to west Rommana (Figure 4). The three areas have different hydrogeological conditions and depositional environments. The coastal aquifer at El-Arish Rafah (Figure 4) is considered to apply the proposed two optimization models with the purpose of

**Table 5** | Comparison between the performances of the two models for Miami Beach

Model/Criteria	Scenario 1		Scenario 2	
	SFLA	PGSL	SFLA	PGSL
$S_r$ %	90	0	70	10
Minimum value	22.75	20.61	4,967.6	4,772.5
Maximum value	24.93	22.8	5,393.5	5,298.2
Mean	24.54	21.97	5,195.6	4,989.4
Standard deviation	0.54	0.52	129.47	116.3
Mean <i>numeval</i>	19,259	3,770	23,654	3,753

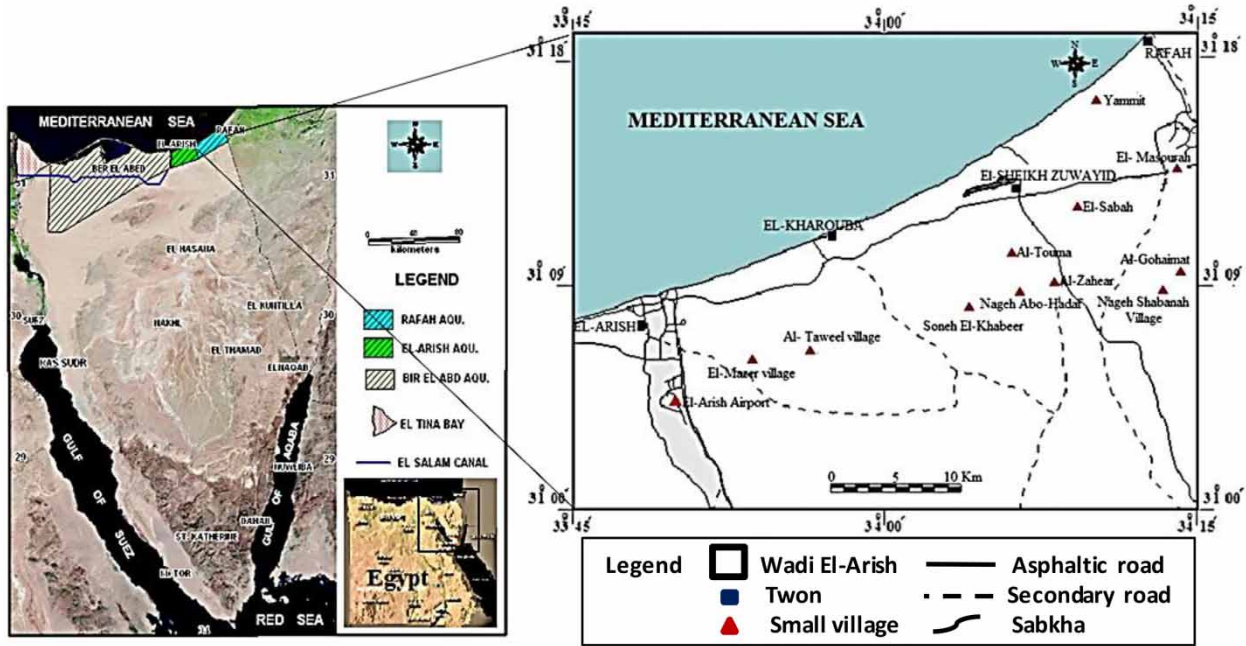


Figure 4 | Map of Sinai Peninsula and location map of El-Arish Rafah area.

maximizing the total pumping rates from a pre-existing system of wells similar to scenario 2 of the model verification.

The lithology of El-Arish Rafah coastal aquifer is grouped into three main units, namely, sand/gravel, clay and Kurkar (i.e. calcareous sandstone). Figure 5 shows a schematic sectional view for the conceptual model of Quaternary aquifer in El-Arish Rafah area. Based on the site characterization, the upper part of the aquifer is sand/gravel (sand dunes, old beach deposits, and alluvial), and the lower part consists of Pleistocene Kurkar formations. In many boreholes the clay layer between the two formations is absent or exists in lenses in which it works as a semi-confining layer for the Kurkar formations (Abdallah 2006). In this study, the coastal aquifer at El-Arish Rafah is considered as shallow and phreatic. Vertical homogeneity is assumed so the three layers have been merged to constitute a single equivalent layer with an equivalent thickness and hydraulic conductivity. Rainfall is the main source of groundwater recharge in the studied area. All hydraulic parameters of the studied aquifer are obtained from the central laboratory of the Desert Research Center, Egypt, and any missing data are reasonably assumed. The length of the aquifer along the shore line ( $Y_D$ ) is 43,200 m and perpendicular to the shore line equals 8,150 m, the equivalent hydraulic conductivity ( $K$ ) is 33 m/d,

the depth of the impervious bed from the M.S.L. ( $d$ ) is 40 m, saltwater density ( $\rho_s$ ) is equal to 1,025 kg/m<sup>3</sup>, and freshwater density ( $\rho_f$ ) is 1,000 kg/m<sup>3</sup>. Both the available point measurements of the flow parameters and hydrological measurements collected by the central laboratory of the Desert Research Center, Egypt, are adopted to calibrate the aquifer recharging flow (El-Sayed 2014). Recharge zones are selected based on the analysis of the colors of a satellite image (Figure 6). Such color composition shows vegetated

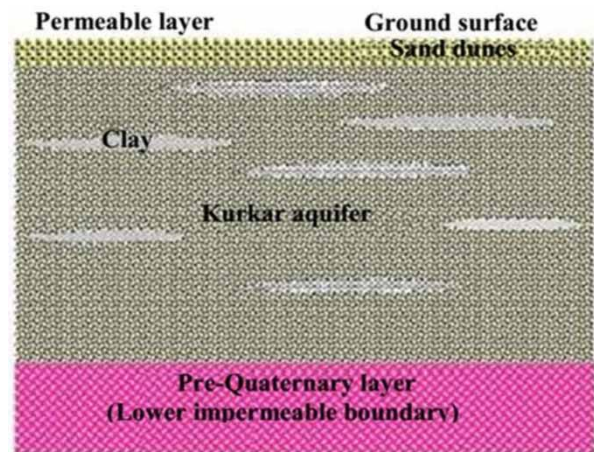


Figure 5 | Schematic section showing the conceptual model of Quaternary aquifer in El-Arish Rafah area.

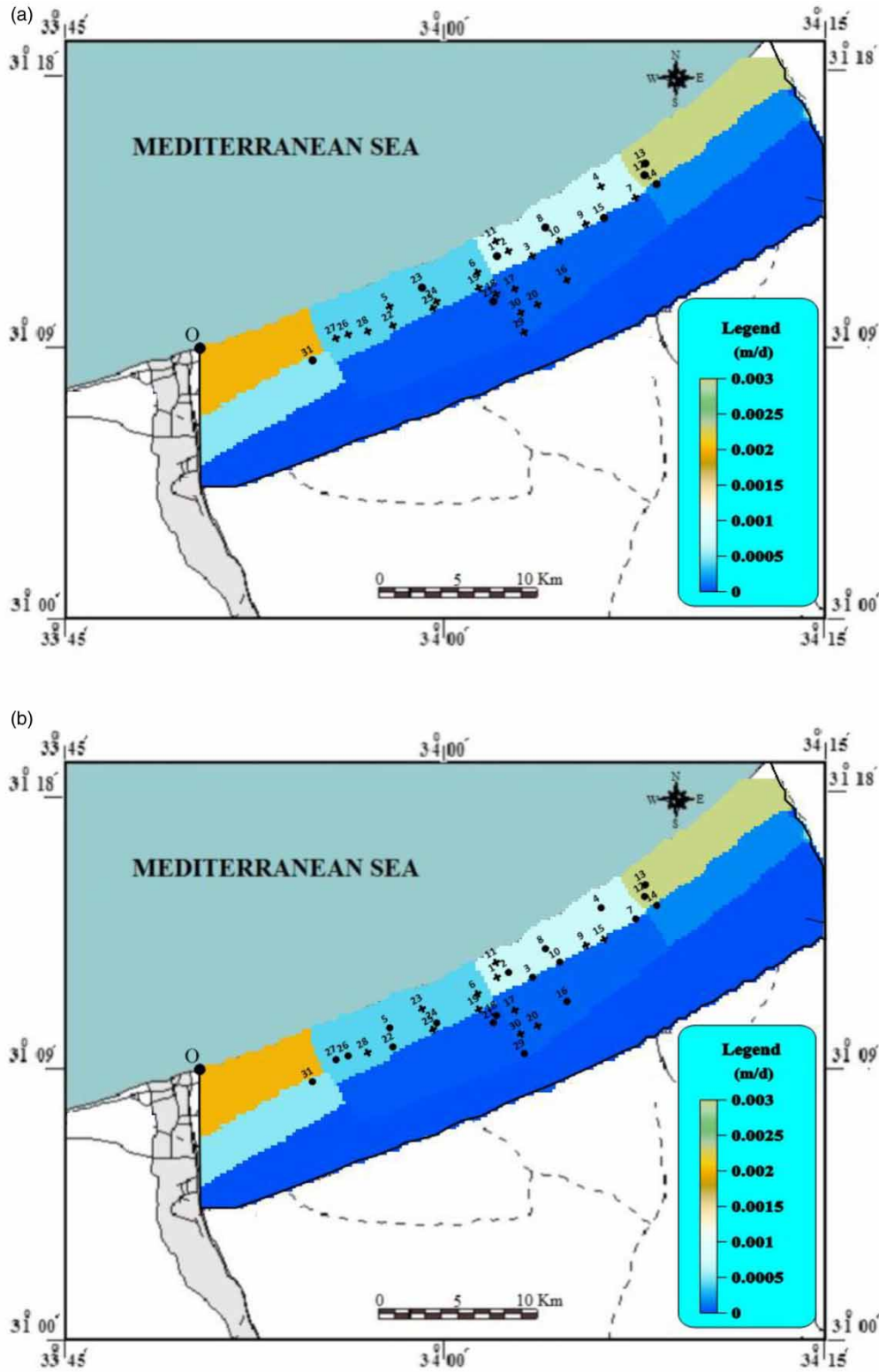


Figure 6 | The locations of wells obtained on the recharging zones map of El-Arish Rafah area. (a) SFLA results. (b) PGSL results.

**Table 6** | The data and results of well system in El-Arish Rafah area

Well no.	X (m)	Y (m)	Max. pumping rate (m <sup>3</sup> /d)	Min. pumping rate (m <sup>3</sup> /d)	Results (pumping rates, m <sup>3</sup> /d)	
					SFLA	PGSL
1	1,864.9	20,783.1	10,000	120	2,376.6	0
2	1,905.5	21,613.4	10,000	120	0	2,324.6
3	2,709.0	23,234.8	10,000	120	0	821.4
4	1,258.5	29,797.2	10,000	120	0	2,781.2
5	1,809.5	12,941.4	10,000	120	0	2,019.6
6	2,052.3	19,414.4	10,000	120	0	0
7	3,223.1	31,268.3	10,000	120	0	1,004.2
8	1,599.7	24,740.9	10,000	120	2,700.1	591.5
9	2,768.2	27,350.1	10,000	120	0	0
10	2,874.1	25,066.1	10,000	120	0	3,312.6
11	673.3	21,374.0	10,000	120	0	0
12	2,226.9	32,504.6	10,000	120	1,222.0	8,374.7
13	1,558.5	33,153.7	10,000	120	7,969.6	2,380.9
14	3,104.7	33,219.8	10,000	120	10,000.0	8,296.4
15	3,104.6	28,897.9	10,000	120	5,105.7	0
16	5,238.3	24,275.0	10,000	120	0	192.0
17	4,504.5	20,781.8	10,000	120	0	0
18	4,087.8	19,815.7	10,000	120	0	276.1
19	3,215.4	18,893.2	10,000	120	0	0
20	5,957.0	21,611.7	10,000	120	0	0
21	4,553.3	19,141.3	10,000	120	2,428.3	2,011.6
22	3,103.6	12,161.8	10,000	120	0	140.1
23	1,534.6	15,314.4	10,000	120	1,059.2	0
24	2,915.7	15,798.2	10,000	120	0	231.4
25	3,238.2	15,388.0	10,000	120	0	0
26	2,423.2	9,345.7	10,000	120	0	298.6
27	2,329.2	8,389.3	10,000	120	0	2,158.7
28	2,771.2	10,616.1	10,000	120	0	0
29	7,206.7	20,177.1	10,000	120	0	120.1
30	5,878.8	20,447.5	10,000	120	0	0
31	3,420.4	6,180.1	10,000	120	10,000.0	9,052.1
Total pumping rates (m <sup>3</sup> /d)					42,861.5	46,387.72

areas where expected returned irrigated water can recharge the aquifer. Calibrated recharge values reflect recharge due to rainfall, returned water from different water uses and possible unknown recharge from other underlying formations are not considered. As shown in Figure 6, the recharge has a maximum value of  $3 \times 10^{-3}$  m/d in the north-east of the study area, while it equals  $1.2 \times 10^{-7}$  m/d

in the southern boundary (Abdallah 2006). Table 6 shows the coordinates of the different pre-existing wells in the aquifer, their allowable maximum and minimum pumping rates, and their corresponding ground level.

In this application, the parameters setting for both the SFLA and the PGSL are summarized in Table 2. After performing several trial runs for each algorithm, the largest

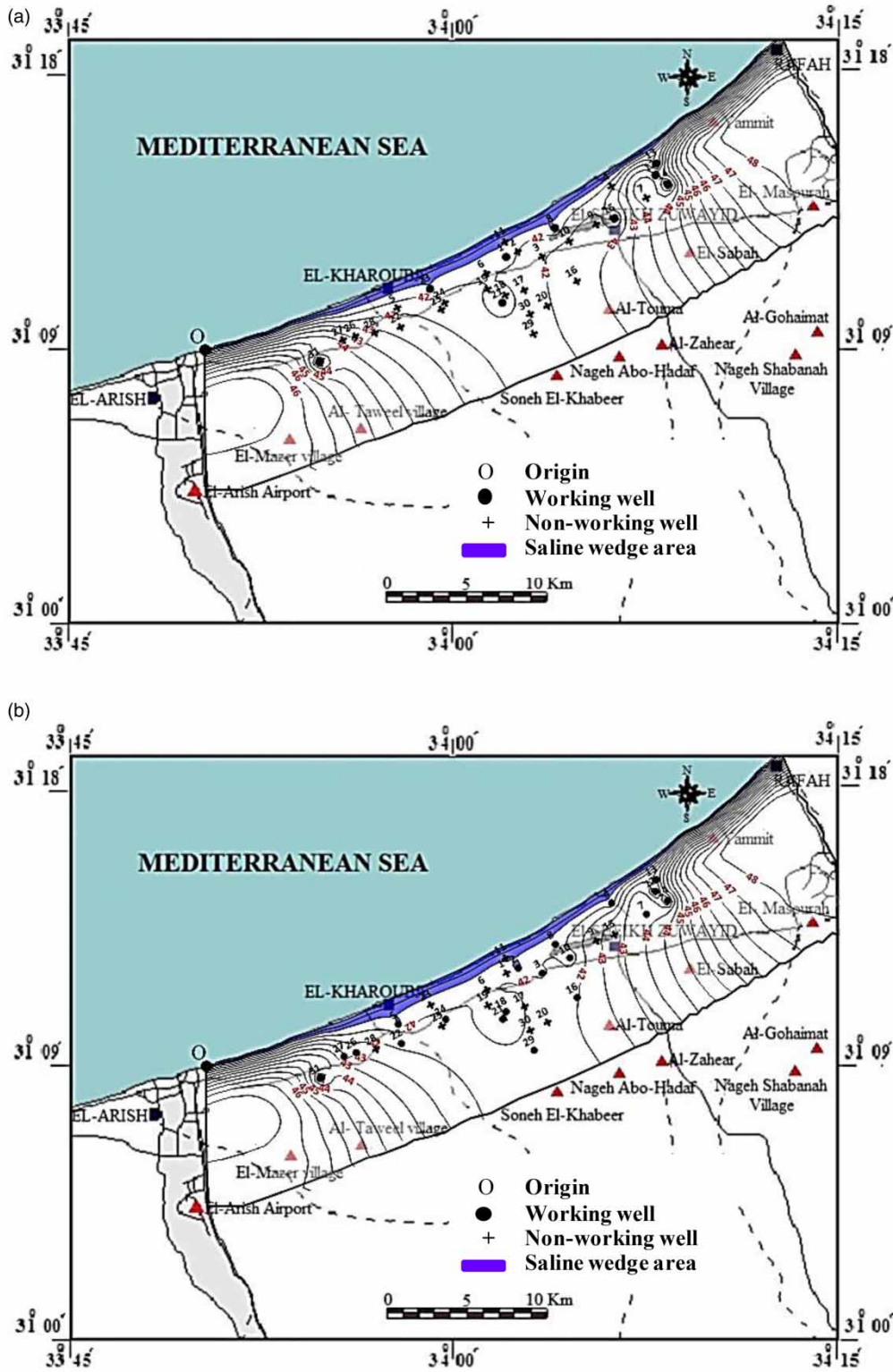


Figure 7 | The contours of water levels measured from impervious bed (in meters) and well system obtained for El-Arish Rafah area. (a) SFLA results. (b) PGSL results.

total pumping rates obtained were 42,861.5 and 46,387.72 m<sup>3</sup>/d, respectively, for both the SFLA and PGSL which represents about 22.1 and 23.9% from the total water entering the aquifer from rainfall. This is due to the non-uniform distribution of wells over the studied domain (the existing wells are not distributed over the whole studied area) and also the number of working wells located in low rainfall recharge zones (Figure 6). The corresponding total numbers of evaluations of the objective function, Equation (1), are 113,133 and 2,000 for the SFLA and PGSL, respectively. From the results obtained, the PGSL outperforms the SFLA and, consequently, the PGSL is more efficient for large scale problems, where the best results are obtained in a smaller runtime of about 35 minutes per one run. Table 6 lists a comparison between well discharges, in each well system, corresponding to the largest total pumping of the two algorithms. Using the SFLA optimization algorithm, the total pumping is obtained from only nine wells out of the 31 wells while 19 worked wells were determined by using the PGSL optimization algorithm.

Figure 7 shows the maps of the water levels contours (measured from the impervious bed) corresponding to each well system listed in Table 6. The locations of the wells have been plotted on the maps. The symbol (●) represents a working well and the symbol (+) represents a non-working well. The shaded areas represent the extent inland of the saline wedge and the contour line corresponding to  $h_{toe} = d \times \rho_s / \rho_f$  at 41 m which represents the sharp interface toe. From the studied aquifer, both the SFLA and PGSL optimization algorithms can be used successfully for management of coastal aquifers with saltwater intrusion.

## CONCLUSIONS

In this study, a probabilistic global search optimization algorithm, namely PGSL, is used along with a hydraulic simulation module to optimize the pumping rates from an unconfined coastal aquifer. The results of the PGSL are compared with the well-known Shuffled Frog Leaping Optimization Algorithm (SFLA). The FEM is applied on the linear formulation of Strack (1976) to simulate the hydraulic response of the steady state homogenous aquifer. A sharp interface between saltwater and freshwater is assumed. The two optimization

algorithms are verified through applying them on the unconfined aquifer beneath Miami Beach to obtain the maximum pumping rate in one scenario and the maximum economic benefit in another scenario and comparisons are carried out with previous studies. Then, statistical analysis is carried out to compare the performance of each optimization algorithm. Both algorithms are then applied on the Quaternary aquifer of El-Arish Rafah, Egypt. The results obtained indicate that the performance of the SFLA is better than the PGSL in terms of the best results obtained. However, the PGSL, which is a relatively new optimization technique, outperformed other traditional stochastic optimization techniques (e.g. the GA). Also, the run time for the PGSL was significantly smaller than the SFLA. The two models can effectively and efficiently be used to solve real groundwater management problems. From the studied aquifers, it is noted that the PGSL does not give the optimum solution but the obtained results are close to the optimum. As such, the PGSL would be a suitable tool in solving large scale problems (i.e. real-life aquifers) to give an initial orientation, not a final decision.

## REFERENCES

- Abarca, E., Vazquez-Sune, E., Carrera, J., Capino, B., Gamez, D. & Batlle, F. 2006 [Optimal design of measures to correct seawater intrusion](#). *Water Resour. Res.* **42**, W09415.
- Abdallah, G. 2006 Management of groundwater aquifers along the Mediterranean Sea in Sinai Peninsula. In: *The 2nd International Conference on Water Resources & Arid Environment*. King Saud University, Riyadh, Saudi, Arabia.
- Abdel-Gawad, H. & Shamaa, M. 2004 Optimal utilization of coastal unconfined aquifers. *Mansoura Eng. J. (MEJ)* **29** (2), C20–C32.
- Abd-Elhamid, F. F. & Javadi, A. A. 2011 [A cost-effective method to control seawater intrusion in coastal aquifers](#). *Water Resour. Manage.* **25**, 2755–2780.
- Adarsh, S. 2012 Design of minimum seepage loss irrigation canal sections using probabilistic search. *Int. J. Optimiz. Civil Eng.* **2** (1), 15–28.
- Adarsh, S. & Sahana, A. S. 2013 [Minimum cost design of irrigation canals using probabilistic global search](#) Lausanne. *Arabian J. Sci. Eng.* **38**, 2631–2637.
- Ataie-Ashtiani, B. & Ketabchi, H. 2011 [Elitist continuous ant colony optimization algorithm for optimal management of coastal aquifers water](#). *Water Resour. Manage.* **25**, 165–190.
- Ataie-Ashtiani, B., Ketabchi, H. & Rajabi, M. M. 2014 [Optimal management of freshwater lens in a small island using surrogate models and evolutionary algorithms](#). *J. Hydrol. Eng. (ASCE)* **19** (2), 339–354.

- Bakker, M. 2003 A Dupuit formulation for modeling seawater intrusion in regional aquifer systems. *Water Resour. Res.* **39** (5), 12-1–12-10.
- Barreto, J., Nuno, M. A. & Haie, N. 2001 Modelling of rural usage of groundwater subject to saltwater intrusion. In: *Proceedings of the 1st International Conference and Workshop on Saltwater Intrusion and Coastal Aquifers, Monitoring, Modelling, and Management (Morocco)*, Essaouira, Morocco.
- Benhachmi, M. K., Ouazar, Z., Naji, A. & Cheng, A. H.-D. 2003 Pumping optimization in saltwater intruded aquifer by simple genetic algorithm-deterministic model. In: *Second International Conference on Saltwater Intrusion and Coastal Aquifers – Monitoring, Modeling and Management*, Merida, Mexico.
- Cheng, A. H. D., Halhal, D., Naji, A. & Ouazar, D. 2000 Pumping optimization in saltwater-intruded coastal aquifers. *Water Resour. Res.* **36** (8), 2155–2166.
- Christelis, V. & Mantoglou, A. 2018 Pumping optimization of coastal aquifers using seawater intrusion models of variable-fidelity and evolutionary algorithms. *Water Resour. Manage.* **33** (2), 555–568.
- El-Alfy, K. S., El-Ghandour, H. A. & Abd-Elmaboud, M. E. 2015 Controlling of saltwater intrusion using injection wells (case study: quaternary aquifer of Delta Wadi El-Arish, Sinai. *Mansoura Eng. J. (MEJ)* **40** (1), C74–C92.
- Elbeltagi, E., Hegazy, T. & Grierson, D. 2007 A modified shuffled frog-leaping optimization algorithm: application to project management. *Struct. Infrastruct. Eng.* **3** (1), 53–60.
- Elçi, A. & Ayvaz, T. M. 2014 Differential-evolution algorithm based optimization for the site selection of groundwater production wells with the consideration of the vulnerability concept. *J. Hydrol.* **511**, 736–749.
- El-Ghandour, H. A. 2005 *Analysis and Optimization of Saltwater Intrusion in Coastal Aquifers*. MSc Thesis, Mansoura University, Egypt, p. 177.
- El-Sayed, M. E. 2014 *Unsteady State Studying of Saltwater Intrusion in Coastal Aquifers*. MSc Thesis, Mansoura University, Egypt, p. 150.
- Emch, P. G. & Yeh, W. W. G. 1998 Management model for conjunctive use of coastal surface water and groundwater. *J. Water. Resour. Plann. Manage. (ASCE)* **124**, 129–139.
- Ferreira da Silva, J. F. & Haie, N. 2007 Optimal locations of groundwater extractions in coastal aquifers. *Water. Resour. Manage.* **21**, 1299–1311.
- Hunt, B. 1983 *Mathematical Analysis of Groundwater Resources*. Butterworth-Heinemann, London, UK, p. 271.
- Javadi, A., Hussain, H., Sherif, M. & Farmani, R. 2015 Multi-objective optimization of different management scenarios to control seawater intrusion in coastal aquifers. *Water Resour. Manage.* **29** (6), 1843–1857.
- Karatzas, G. P. & Dokou, Z. 2015 Optimal management of saltwater intrusion in the coastal aquifer of Malia, Crete (Greece), using particle swarm optimization. *Hydrogeol. J.* **23**, 1181–1194.
- Katsifarakis, K. L. & Petala, Z. 2006 Combining genetic algorithms and boundary elements to optimize coastal aquifers management. *J. Hydrol.* **327**, 200–207.
- Katsifarakis, K. L. & Tselepidou, K. 2009 Pumping cost minimization in aquifers with regional flow and two zones of different transmissivities. *J. Hydrol.* **377** (1–2), 106–111.
- Kopsiaftis, G., Christelis, V. & Mantoglou, A. 2017 Pumping optimization in coastal aquifers: comparison of sharp interface and density dependent models. *European Water* **57**, 443–449.
- Kopsiaftis, G., Christelis, V. & Mantoglou, A. 2019 Comparison of sharp interface to variable density models in pumping optimisation of coastal aquifers. *Water Resour. Manage.* **33** (4), 1397–1409.
- Kourakos, G. & Mantoglou, A. 2009 Pumping optimization of coastal aquifers based on evolutionary algorithms and surrogate modular neural network models. *Adv. Water Resour.* **32**, 507–521.
- Kourakos, G. & Mantoglou, A. 2011 Simulation and multi-objective management of coastal aquifers in semi-arid regions. *Water. Resour. Manage.* **25**, 1063–1074.
- Ma Tain, S., Sophocleous, M., Yu, Y. & Buddemeier, R. W. 1997 Modelling saltwater upconing in a freshwater aquifer south-central Kansas. *J. Hydrol.* **201**, 120–137.
- Ojeda, C. G., Gallardo, P., Hita, L. G. & Arteaga, L. M. 2004 Saline interface of the Yucatan Peninsula aquifer. In: *Proceedings of the 18th Salt Water Intrusion Meeting*, Cartagena, Spain.
- Oude Essink, G. H. P. 2001 Saltwater intrusion in 3D large-scale aquifers: a Dutch case. *Phys. Chem. Earth B* **26**, 337–344.
- Paniconi, C., Khlaifi, I., Lecca, G., Giacomelli, A. & Tarhouni, J. 2001 A modelling study of seawater intrusion in the Korba Plain, Tunisia. *Phys. Chem. Earth B* **26** (4), 345–351.
- Rao, S. V. N., Sreenivasulu, V., Bhallamudi, S. M., Thandaveswara, B. S. & Sudheer, K. P. 2004 Planning groundwater development in coastal aquifers. *Hydrol. Sci. J.* **49**, 155–170.
- Raphael, B. & Smith, I. F. C. 2003a A probabilistic search algorithm for finding optimally directed solutions. In: *Proceedings of Construction and Information Technology*. Iceland Building Research Institute, Reykjavik, Iceland, pp. 708–721.
- Raphael, B. & Smith, I. F. C. 2003b A direct stochastic algorithm for global search. *Appl. Math. Comput.* **146** (3), 729–758.
- Scholze, O., Hillmer, G. & Schneider, W. 2002 Protection of the groundwater resources of metropolis CEBU (Philippines) in consideration of saltwater intrusion into the coastal aquifer. In: *Proceedings of the 17th Salt Water Intrusion Meeting*, Delft, The Netherlands.
- Strack, O. D. L. 1976 A single-potential solution for regional interface problems in coastal aquifers. *Water Resour. Res.* **12**, 1165–1174.
- Yang, Y., Wu, J., Lin, J., Wang, J., Zhou, Z. & Wu, J. 2018 An efficient simulation–optimization approach for controlling seawater intrusion. *J. Coast. Res.* **84**, 10–18.
- Zhou, X., Chen, M. & Liang, C. 2003 Optimal schemes of groundwater exploitation for prevention of seawater intrusion in the Leizhou Peninsula in southern China. *Environ. Geol.* **43**, 978–985.